Improved predictions of reactor antineutrino spectra

Th. A. Mueller,[1] D. Lhuillier,[1,*] M. Fallot,[2] A. Letourneau,[1] S. Cormon,[2] M. Fechner,[3] L. Giot,[2] T. Lasserre,[3] J. Martino,[2] G. Mention,[3] A. Porta,[2] and F. Yermia[2]

[1]*Commissariat à l'Énergie Atomique et aux Énergies Alternatives, Centre de Saclay, IRFU/SPhN, FR-91191 Gif-sur-Yvette, France*

[2]*Laboratoire SUBATECH, École des Mines de Nantes, Université de Nantes, CNRS/IN2P3, 4 rue Alfred Kastler, FR-44307 Nantes Cedex 3, France*

[3]*Commissariat à l'Énergie Atomique et aux Énergies Alternatives, Centre de Saclay, IRFU/SPP, FR-91191 Gif-sur-Yvette, France*

(Received 14 December 2010; revised manuscript received 9 March 2011; published 23 May 2011)

Precise predictions of the antineutrino spectra emitted by nuclear reactors is a key ingredient in measurements of reactor neutrino oscillations as well as in recent applications to the surveillance of power plants in the context of nonproliferation of nuclear weapons. We report new calculations including the latest information from nuclear databases and a detailed error budget. The first part of this work is the so-called *ab initio* approach where the total antineutrino spectrum is built from the sum of all β branches of all fission products predicted by an evolution code. Systematic effects and missing information in nuclear databases lead to final relative uncertainties in the 10–20% range. A prediction of the antineutrino spectrum associated with the fission of ^{238}U is given based on this *ab initio* method. For the dominant isotopes we developed a more accurate approach combining information from nuclear databases and reference electron spectra associated with the fission of ^{235}U, ^{239}Pu, and ^{241}Pu, measured at Institut Laue-Langevin (ILL) in the 1980s. We show how the anchor point of the measured total β spectra can be used to suppress the uncertainty in nuclear databases while taking advantage of all the information they contain. We provide new reference antineutrino spectra for ^{235}U, ^{239}Pu, and ^{241}Pu isotopes in the 2–8 MeV range. While the shapes of the spectra and their uncertainties are comparable to those of the previous analysis of the ILL data, the normalization is shifted by about +3% on average. In the perspective of the reanalysis of past experiments and direct use of these results by upcoming oscillation experiments, we discuss the various sources of errors and their correlations as well as the corrections induced by off-equilibrium effects.

DOI: 10.1103/PhysRevC.83.054615 PACS number(s): 23.40.−s, 28.41.Ak, 14.60.Pq, 28.41.Te

I. INTRODUCTION

Nuclear power plants are the most intense man-controlled sources of neutrinos. With an average energy of about 200 MeV released per fission and six neutrinos produced along the β-decay chain of the fission products, one expects some 2×10^{20} ν/s emitted in a 4π solid angle from a 1 GW reactor (thermal power). Since unstable fission products are neutron-rich nuclei, all β decays are of β^- type, and the neutrino flux is actually pure electronic antineutrinos ($\bar{\nu}_e$). These unique features have been exploited by several neutrino oscillation experiments [1,2]. Improvement in the accuracy of $\bar{\nu}_e$ spectra is motivated by next generation experiments [3–5] aiming at unprecedented sensitivity to the last unknown mixing angle θ_{13}. The value of this parameter may determine the future trend of neutrino physics, in particular for the search of charge conjugation and parity (CP) violations in the lepton sector. Recent developments of compact (1 m^3 target scale) $\bar{\nu}_e$ detectors as new safeguard tools for the monitoring of reactors [6–8] would also benefit from an accurate description of $\bar{\nu}_e$ spectra.

In a reactor core, only one neutron among the few generated by the fission of a ^{235}U nucleus should induce another fission, so that the core never reaches the over-critical regime. A fraction of the neutrons is actually captured by the dominant ^{238}U isotope leading to the production of new fissile isotopes: ^{239}Pu and to a lesser extent ^{241}Pu. When operating, a core is thus burning ^{235}U and accumulating ^{239}Pu. This is the so-called burnup process. In a pressurized water reactor, fission rates from both isotopes become comparable at the end of a cycle. The remaining fissions of ^{241}Pu and fast neutron induced fissions of ^{238}U share about 10% of the reactor power. As a result, the accurate prediction of the $\bar{\nu}_e$ spectrum of a reactor requires following the time evolution of these four isotopes, as well as the knowledge of the associated β spectra of their neutron-rich fission products.

This paper presents an improved treatment of the latter piece of information, common to the prediction of the $\bar{\nu}_e$ spectrum of any moderated reactor. This work was triggered by the current effort of precision measurement of reactor neutrinos in the Double Chooz Collaboration [3]. Our approach combines the assets of the two main methods used so far. The first method is the so-called *ab initio* approach where the $\bar{\nu}_e$ spectrum associated with one of the four fissioning isotopes is computed as the sum of the contributions from all fission products. This requires a huge amount of information on the thousands of β branches involved and the weighting factors of fission products, the fission yields. Section II presents details on the ingredients of the *ab initio* approach, while Sec. III gives an update of *ab initio* calculations combining all data available today. The main systematic errors are discussed, and a prediction of ^{238}U spectra is given since this isotope is the only one with no integral β spectrum measured yet.

The second method relies on reference electron spectra [9–12] measured at the high flux Institut Laue-Langevin

*Corresponding author: david.lhuillier@cea.fr

(ILL) reactor in Grenoble (France) using a high-resolution magnetic spectrometer [13]. It is presented in Sec. IV where we explain how these electron spectra are converted into antineutrino spectra with incomplete knowledge of the underlying physical distribution of β branches. We show how our "mixed-approach" can improve the control of systematic errors and lead to a significant correction of the reference neutrino spectra used by all oscillation experiments so far. Finally we discuss in Sec. V our results in the context of neutrino reactor experiments.

II. INGREDIENTS OF REACTOR SPECTRA

In the present work we describe the total β spectrum emitted by a reactor as the sum of the contributions from the four fissioning nuclei mentioned in Sec. I

$$S_{\text{tot}}(E) = \sum_{k=^{235}\text{U},^{238}\text{U},^{239}\text{Pu},^{241}\text{Pu}} \alpha_k S_k(E), \tag{1}$$

where α_k is the number of fissions of the kth isotope at the considered time, $S_k(E)$ is the corresponding β spectrum normalized to one fission, and E is the kinetic energy of emitted electrons.

Most of the equations below can be found in textbooks, but they are useful here to define our notations and discuss the systematic errors in the following sections. In the *ab initio* approach, $S_k(E)$ is broken up into the sum of contributions from all fission products, i.e.,

$$S_k(E) = \sum_{f=1}^{N_f} \mathcal{A}_f(t)\, S_f(E), \tag{2}$$

where $\mathcal{A}_f(t)$ is the activity of the fth fission product at time t and normalized to one fission of isotope k. Then the spectrum $S_f(E)$ of each fission product is itself a sum of N_b β branches connecting the ground state (or in some cases an isomeric state) of the parent nucleus to different excited levels of the daughter nucleus

$$S_f(E) = \sum_{b=1}^{N_b} \text{BR}_f^b \;\; S_f^b(Z_f, A_f, E_{0f}^b, E), \tag{3}$$

where BR_f^b and E_{0f}^b are the branching ratio and the endpoint energy of the bth branch of the f^{th} fission product, respectively. Z_f and A_f are the charge and atomic number of the parent nucleus. The sum of the branching ratios is normalized to the β-decay partial width of the parent nucleus (1 if the parent is a pure β^- emitter, <1 otherwise).

Equations (1)–(3) are valid for both electron and antineutrino spectra. The expression of the electron spectrum of the bth branch is given by the product of the following terms:

$$S_f^b = \underbrace{K_f^b}_{\text{Norm.}} \times \underbrace{\mathcal{F}(Z_f, A_f, E)}_{\text{Fermi function}} \times \underbrace{pE\left(E - E_{0f}^b\right)^2}_{\text{Phase space}} \times \underbrace{C_f^b(E)}_{\text{Shape factor}} \times \underbrace{\left(1 + \delta_f^b(Z_f, A_f, E)\right)}_{\text{Correction}}. \tag{4}$$

To obtain the corresponding expression for the antineutrino spectrum, one can safely neglect the nucleus recoil and replace in the above formula the electron energy E by the antineutrino energy

$$E_\nu = E_{0f}^b - E. \tag{5}$$

By definition this one-to-one relation is valid only at the single β-branch level. Thus this is a unique feature of the *ab initio* approach to predict electron and antineutrino spectra with the same precision. The normalization factor K_f^b of Eq. (4) is calculated so that the integral $\int_0^{E_0} S_f^b(E)\, dE = 1$. Hence the contribution to the integral of $S_f(E)$ is driven by the branching ratio, as it should be. The next two terms come from the Fermi theory. The Fermi function $\mathcal{F}(Z_f, A_f, E)$ corrects for the deceleration of the electron in the Coulomb field created by the $Z_f \times e$ positive charge of the parent nucleus. Therefore in the case of β^- decay, the Fermi function causes the electron spectrum to start at a nonzero value at zero kinetic energy. This corresponds to a sharp step at the endpoint energy for the antineutrino spectrum, leading to discontinuities when summing several branches of different endpoints.

The shape factor $C_f^b(E)$ brings extra energy dependence beyond the trivial phase space factor of the Fermi theory, due to the nuclear matrix element connecting the two nuclear levels of the β decay. Its complexity depends on the forbiddenness of the transition, driven by the spin-parity of the connected levels. In the case of allowed transitions, $C_f^b(E)$ is a constant and is absorbed in the normalization factor.

For accurate predictions one must also take into account corrections, represented by the δ_f^b factor in Eq. (6). This term is threefold

$$\delta_f^b(Z_f, A_f, E) = \delta_{\text{QED}}(E) + A_C(Z_f, A_f)E + A_W E. \tag{6}$$

The δ_{QED} term corrects for radiation of real and virtual photons by the charged fermion lines of the β-decay vertex. Its expression has been calculated at order α_{QED} by Sirlin *et al.* [14]. The fact that only the charged fermions radiate photons implies that the δ_{QED} formula differs for electron and antineutrino spectra, the electron spectrum deviating more from the shape predicted by lowest order calculation than that of the antineutrino. Strictly speaking, Eq. (5) now becomes $E_0 = E_e + E_\nu + E_\gamma$, where E_γ represents the energy of the radiated photon. Still the E_γ spectrum goes like $1/E_\gamma$ and the dominant contribution comes from soft ($E_\gamma \ll E_0$) radiated photons. Therefore the total energy of the lepton pair remains very close to E_0. The physical constraint of conservation of the number of particles is fulfilled by the equality

$$\int_0^{E_0} S_f^b(E_e)\left[1 + \delta_{\text{QED}}^e(E)\right] dE_e = \int_0^{E_0} S_f^b(E_\nu)\left[1 + \delta_{\text{QED}}^\nu(E)\right] dE_\nu, \tag{7}$$

which we verified numerically. The A_C term is a Coulomb correction induced by the finite size of the decaying nucleus. It is related to the interference of $\langle\vec{\sigma}\rangle$ and $\langle\vec{\sigma}\cdot\vec{r}^{\,2}/R^2\rangle$ matrix elements, where R is the nuclear radius and $\vec{\sigma}$ the spin operator.

In the following we use the approximate expression derived by Vogel [15]:

$$A_C = -\frac{10}{9}\frac{Z\alpha R}{\hbar c} \tag{8}$$

and the Elton formula [16] as an estimate of nuclear radii.

The nucleon itself also has a finite size, and as a consequence the expression of its weak current deviates from that of a point-like particle. The complex effects of the nucleon internal structure can be absorbed in the definition of factors in front of each term of the most general nucleon weak current allowed by the symmetries of the theory. The equivalent in the electromagnetic sector is the introduction of the Pauli (F_1) and Dirac (F_2) form factors of the nucleon, with the F_2 contribution proportional to the momentum transfer. The A_W term contains the conserved vector current (CVC) partner contribution of F_2 in the vector weak current and is called the weak magnetism correction. Again we choose as a reference expression the one derived by Vogel [15]

$$A_W = -\frac{4}{3}\frac{\kappa_p - \kappa_n - 1/2}{M_N \lambda}, \tag{9}$$

with $\lambda = g_A/g_V = -1.2695$ the neutron disintegration constant and $M_N = 939$ MeV the nucleon mass. One recognizes the $(\kappa_p - \kappa_n)/M_N$ term proportional to F_2 at small ($\ll M_N^2$) square momentum transfer. Other expressions of A_C and A_W can be found in the literature [17]. The associated uncertainty is large and amplified by a sign compensation between the two terms. The net effect of these finite size corrections and its final error are discussed in Secs. III and IV.

III. *AB INITIO* COMPUTATION OF β SPECTRA FROM FISSION FRAGMENTS

A. Selection of the best data set

In principle, the ultimate prediction of the $S_k(E)$ spectra comes from the knowledge of all quantities involved in Eqs. (2)–(4). The first attempts at such an *ab initio* approach were theoretical [18–21]. Most of these calculations use rather crude models to describe the hundreds of involved nuclei, but their goal is a correct description of total fission spectra $S_k(E)$, not individual β transitions.

Efforts have also been made recently in comparing microscopic models, mostly theoretical models based on the quasiparticle random-phase approximation (QRPA) and the nuclear shell model, in the framework of double-β-decay studies [22]. Whereas these microscopic models are the ones susceptible to giving the most reliable predictions, they are still difficult to apply to large sets of nuclei, especially heavy nuclei (such as the large mass region of the fission products) because of the large model spaces required. The estimation of the error associated with theoretical predictions remains a difficult task, and in practice they have been supplanted by measurements performed in the 1980s at the ILL high flux reactor in Grenoble [9–12]. Only the ^{238}U spectrum remains calculated [20,23], since no related data exist yet. Nevertheless a measurement in the fast neutron flux of the FRM II reactor in Garching, Germany, has lately been performed [24] and should be published soon.

We describe here a complementary *ab initio* approach with the strategy of exploiting all data available in modern nuclear databases while reducing the input of nuclear models. The total spectrum $S_k(E)$ of each fissioning isotope is built up according to the equations of Sec. II, retrieving the information on all β branches from the Evaluated Nuclear Structure Data File (ENSDF) nuclear database [25]. The motivations for such an approach are that when all parameters of a β branch are known, the neutrino branch is also known in a model-independent way and all errors on the input parameters can in principle be propagated. We have developed an interface with the ENSDF data library to read the relevant parameters of Eqs. (3) and (4) and their experimental error. The forbiddenness of a β transition is deduced from the spin and parity of the connected nuclear levels. In cases when this information is missing or uncomplete, the lowest possible forbiddenness is chosen by default. All transitions tagged as forbidden are then forced to be of a unique type, and the corresponding expressions of the shape factors $C_f^b(E)$ are polynomials in the electron and antineutrino momenta taken from Ref. [26]. Using our homemade code BESTIOLE, all the above approximations used for the calculation of each branch are tagged and various scenarios can be tested to estimate the error envelope of the final predicted spectrum. From Eqs. (3) and (4), the electron and antineutrino spectra of each fission product are computed and stored in a database.

Then the total β spectrum of one fissioning isotope is built as the sum of all fission fragment spectra weighted by their activity [Eq. (2)]. These activities are determined using a simulation package called MCNP Utility for Reactor Evolution (MURE [27]). MURE is a precision code written in C++ which automates the preparation and computation of successive MCNP (Monte-Carlo N-Particle transport code [28]) calculations either for precision burnup or thermal-hydraulics purposes. It is open source, portable, and available from the Nuclear Energy Agency [29] and it constitutes an efficient tool for nonproliferation and thermal power scenario studies (for more details, see Ref. [30]).

The detection process, common to many reactor antineutrino experiments, is the β-inverse reaction on a free proton

$$\bar{\nu}_e + p \rightarrow e^+ + n, \tag{10}$$

which sets an energy threshold for the antineutrino of 1.804 MeV, the mass difference between the initial and final states (see Fig. 1). Therefore the lowest energy part of the β spectra, below this threshold, is not addressed here. In this region, equilibrium is reached only after several months, requiring the control of significant transient effects when considering shorter irradiation times. Extra effects such as the low energy β decays induced by neutron capture on ^{238}U and fission products [31] would also have to be treated. On the high energy side, antineutrino rates above 8 MeV become negligible ($<0.5\%$ of total detected rate). This part of the spectrum is dominated by the very energetic (high Q_β) transitions of rare exotic nuclei and cannot be accurately predicted. Thus the intermediate energy range resulting from the observation of the detected spectrum in Fig. 1 turns out to be favorable to the

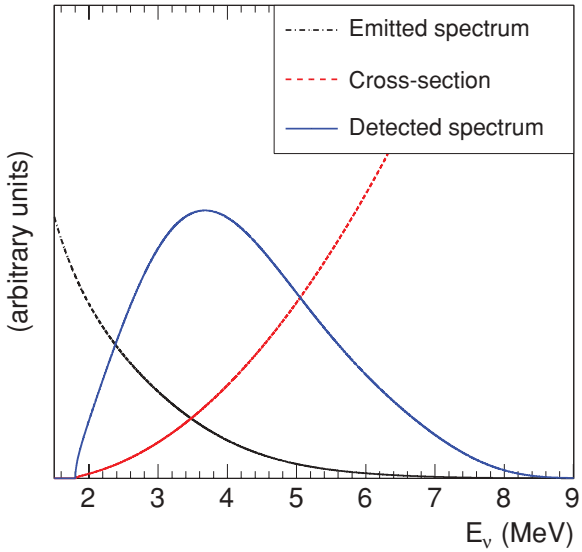

FIG. 1. (Color online) Detected antineutrino spectrum for ^{235}U fission (blue solid curve). Units are arbitrary and oscillation effects are suppressed. The detected rate rises from the threshold value at about 1.8 MeV, reaches a maximum around 4 MeV, and vanishes after 8 MeV. This shape is the result of folding the emitted spectrum (black dashed-dotted curve), parametrization taken from Sec. V A and β-inverse cross section (red dashed curve).

control of the systematic errors of the predictions of reactor antineutrino spectra.

A powerful test of our calculations is the comparison with the reference electron spectra from ILL [10–12]. Such a consistency check gives valuable insight into the distribution of the numerous β branches, pointing to the main source of errors in the determination of the antineutrino spectra. Considering all the data available in the ENSDF data library, the predicted β spectra associated with the fission of ^{235}U and ^{239}Pu are compared with the reference ILL data in Fig. 2.

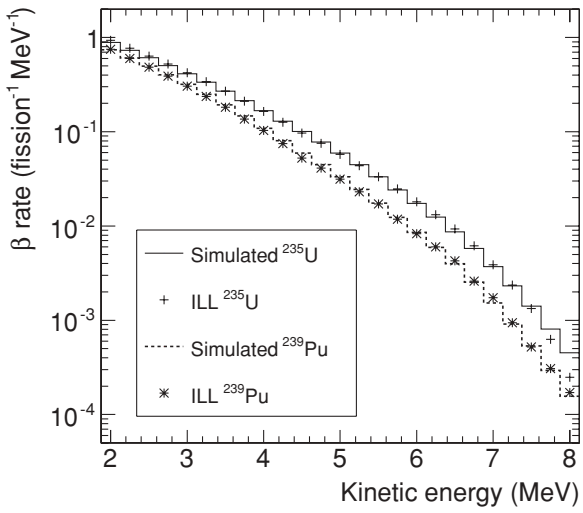

FIG. 2. Comparison of ^{235}U and ^{239}Pu reference electron spectra from Refs. [10,11] with our predictions based on the *ab initio* approach. The predictions have no free parameters, and the rates are normalized to one fission.

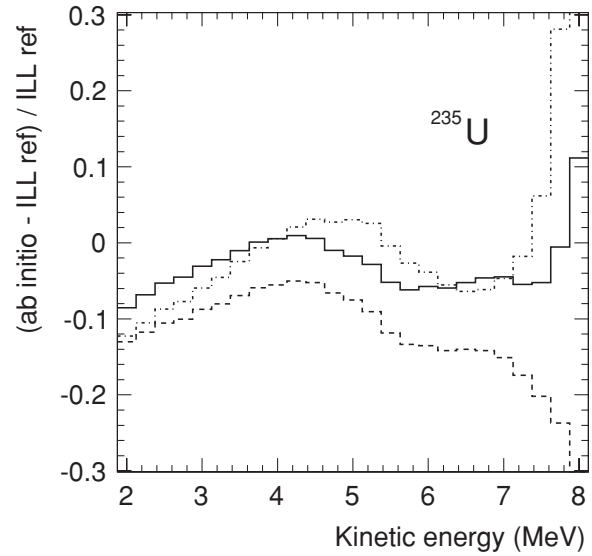

FIG. 3. Residues of the ^{235}U electron spectra computed as the difference of our *ab initio* calculations minus reference data from Ref. [10] divided by reference data. Dashed-dotted curve: ENSDF data only; dashed curve: some ENSDF data replaced by pandemonium corrected data; solid curve: unmeasured β emitters are added on top of the previous curve, using the gross-theory calculations of the JENDL nuclear database and a few remaining exotic nuclei described by our model (see text).

Although the spectrum falls quickly with energy, reasonable agreement is found on the shape and absolute normalization over a quite large energy range. Note that our prediction is parameter free. For finer analysis the residues of our predicted ^{235}U spectrum with respect to reference data are shown as the dashed-dotted line in Fig. 3. It reveals a $\pm 10\%$ oscillation pattern of the calculations around the data up to 7.5 MeV and a large overestimation at higher energy. This overestimation points to the well-known systematic effect of pandemonium [32]. Indeed branching ratios and endpoints are usually determined by measuring the intensity and energy of γ radiations emitted subsequently to the β transition using high resolution but low efficiency Ge crystals. In the case of large Q_β, a fraction of the β branches connects the parent nucleus to very excited levels of the daughter nucleus. The strength of the associated low energy β rays is either spread over multiple weak γ rays or concentrated in one high energy γ ray. In both cases, part or all the γ cascade can be missed by the measurement apparatus. As a result, low endpoint transitions are often missed and high endpoints are given too much weight in the global decay scheme of the parent nucleus.

To correct for the pandemonium effect, we tried to gather β-decay data using other experimental techniques than the β-γ coincidence. A valuable set of data comes from the measurement campaign undertaken by Tengblad *et al.* [33] in the late 1980s at the on-line isotopes separators ISOLDE, at CERN, Geneva, and OSIRIS at the Neutron Research Laboratory, Studsvik. Some 111 fission products, selected as the main contributors to the high energy part of reactor β spectra (90% above 6 MeV) were measured. Electron spectra were recorded independently from the emitted γ rays. This

prevented sensitivity to the pandemonium effec, but at the same time, part of the information on single β branches was lost. Among the 111 measured electron spectra, 44 were found in perfect agreement with the spectra predicted from the ENSDF database. The remaining 67 were then replaced in our database.

Another important source of data are the measurements based on total absorption γ spectrometers (TAGS). The principle here is to implant the radioactive isotope on a foil surrounded by high efficiency γ detectors capable of collecting the whole γ cascade following the β decay. The distribution of total γ energies gives access to the β strength of the studied isotope at the cost of a deconvolution analysis taking into account the full response of the apparatus. Eventually a complete β-decay scheme can be determined providing the relevant β-branch information for electron and antineutrino spectra. Thus the 29 nuclei of Greenwood *et al.* [34] measured at the Idaho National Laboratory were incorporated into our database. Algora and Tain studied carefully both the Tengblad *et al.* and Greenwood *et al.* measurements [35]. Both may have been affected by several sources of systematic effects which are difficult to quantify. In particular, both measurements of ^{91}Rb β decay mean energy differ by more than 350 keV, while the ^{91}Rb decay scheme was used in Tengblad *et al.*'s analysis to quantify the γ-ray detector's absolute efficiency. If the ^{91}Rb decay scheme is affected by the pandemonium effect, Tengblad *et al.*'s data sets may exhibit an overall systematic effect. A new TAGS measurement of the decay properties of ^{91}Rb has recently been performed at the Jyväskylä University facility [36] and will help address the uncertainties associated with both sets of measurements. In cases when a fission product was present in both data sets (eight nuclei only), giving the priority to the Greenwood *et al.* or Tengblad *et al.* measurements changes the predicted spectrum by 3% at most in the 4–5 MeV range, the effect drops at the 1% level or below elsewhere.

In the following, priority is arbitrarily given to the Tengblad *et al.* data. The dashed line in Fig. 3 shows the electron residues after merging our ENSDF-based database with the above selected spectra supposedly corrected for the pandemonium effect. As expected the high energy part of our prediction has been significantly reduced, leading to negative residues of increasing amplitude with energy. This indicates that a large part of the pandemonium effect is probably corrected and that contributions from the missing unknown transitions of exotic nuclei grow rapidly with energy.

To fill up this missing contribution, we collected all available predictions of electron spectra from the Japanese Evaluated Nuclear Data Library (JENDL) [37]. These predictions are based on the "Gross Theory of Beta Decay" [38] and were included in the JENDL database to supplement ENSDF data showing incomplete level schemes or for nuclei for which no data were available. The estimated spectra were stored in the JENDL file so as to keep the consistency between the average decay energy value derived from the spectrum and that used for decay heat analysis [39]. The calculated spectra were also compared with the directly measured spectra from Ref. [33] and revealed to be in very good agreement. The total contribution of the JENDL electron spectra, not already included in the ENSDF and pandemonium corrected data, was computed and converted to its associated total antineutrino spectrum following the procedure described in Ref. [10]. Finally the few remaining nuclei were described using a model based on fits of the distributions of the endpoints and branching ratios in the ENSDF database, then extrapolated to the exotic nuclei. The result is the solid curve in Fig. 3 showing flattened residues within a global envelope of $\pm 10\%$ over the whole energy range. This best agreement with the ILL reference data is actually valid for the ^{239}Pu isotope. Depending on the considered fissioning isotope, this new compilation of β-decay data includes about 845 nuclei and 10 000 β branches, about 525 nuclei come from the ENSDF and pandemonium corrected data, 285 from the JENDL database, and 35 from our model. It represents the best data set for *ab initio* calculations.

B. Results

From this work we conclude that a compilation of all available data on the β decays of fission products can describe the antineutrino fission spectra at the 10% level, illustrating the tremendous experimental work already achieved. Still, the relatively large energy range of detected antineutrino involves a sizable contribution of unstable and poorly known nuclei in the total spectrum. Under these conditions, improving errors or even reaching the accuracy of the ILL reference spectra seems to require another fair amount of experimental effort. For applications like the determination of reactor decay heat calculations, a short list of "pandemonium candidates" to be remeasured with total absorption techniques has been identified [40]. Completion of a corrected β-decay database is in progress (see, for instance, [41]) with more and more refined analyses [42].

Thanks to our database of fission product spectra, we have established a list of nuclei contributing importantly to different energy bins of the antineutrino energy spectra from ^{235}U and ^{239}Pu, and which could be affected by the pandemonium effect. It will be the subject of a forthcoming publication. From this list we have selected a few nuclei which are amenable to experimental investigation using the TAGS technique, which can provide the β-intensity distribution in the full decay window eliminating the pandemonium effect. It appeared that some fission products that are part of the measurement priority list selected for reactor decay heat assessment [41] also belong to the list of important contributors to the antineutrino emission in the energy window of interest for neutrino oscillation studies. Recent and ongoing experimental efforts carried out in the field of reactor physics and neutrino physics but also of interest for nuclear structure and astrophysics will certainly allow a reduction in the uncertainties associated with the reactor antineutrino spectra computed through the *ab initio* method in the very next few years [36,41,43,44]. We describe below the estimated error budget of our *ab initio* calculations and give a prediction of electron and antineutrino spectra of ^{238}U. In the perspective of neutrino oscillation analyses, the ^{235}U and ^{239}Pu isotopes, which contribute to about 90% of a nuclear reactor spectrum, are predicted using a more accurate method presented in Sec. IV.

TABLE I. Correlation matrix in the range 2 to 3.5 MeV in 250 keV bins obtained by propagating all sources of errors in ENSDF and JEFF databases. Branching-ratio errors cause a very high level of correlation then reduced by the endpoint distribution and assumption of independent fission yields.

$$\rho = \begin{pmatrix} 1 & 0.54 & 0.48 & 0.41 & 0.38 & 0.34 & \dots \\ 0.54 & 1 & 0.48 & 0.43 & 0.39 & 0.35 & \\ 0.48 & 0.48 & 1 & 0.46 & 0.42 & 0.38 & \\ 0.41 & 0.43 & 0.46 & 1 & 0.42 & 0.39 & \\ 0.38 & 0.39 & 0.42 & 0.42 & 1 & 0.39 & \\ 0.34 & 0.35 & 0.38 & 0.39 & 0.39 & 1 & \\ \dots & & & & & & \end{pmatrix}$$

C. Error budget

As mentioned earlier, the control of the parameters of all single β branches allows a full propagation of the errors quoted in the ENSDF database. All sources of error are treated as independent, and the total error matrix of rates in energy bins is computed. In the simpler case of a spectrum at equilibrium, the activity of each fission product is approximated by the associated cumulative fission yield indexed in the JEFF3.1.1 database [45]. Then the uncertainty in branching ratios and fission yields can be propagated analytically, while the uncertainty in endpoints is propagated numerically (it turns out to have a negligible contribution). The dominant contribution of normalization errors induces large correlations between proximate bins as illustrated in Table I. Note that these correlations are valid only for the specific part of the measurement errors quoted in the nuclear databases. As summarized in Table II, we know from the above section that systematic effects beyond these databases are dominant and will change these correlations in a nontrivial way as long as all β branches are not corrected.

The second column of Table II lists the global effect of the errors quoted in ENSDF at the 1σ level. It rises from 1 to 10% in the 2–8 MeV range. Columns 3 and 4 show the impact of the theoretical assumptions used to describe the shape of the β branches. Previous works always treated all branches as allowed. Comparing this hypothesis with our full treatment of forbiddenness shows changes of the final antineutrino spectrum below the 1% level (except for a few bins around 4 MeV), validating the allowed approximation. The error associated with the finite size corrections A_C and A_W has been estimated by comparing the final spectra computed with no correction and those with the corrections from Vogel [15] or Holstein [17]. The missing information on exotic nuclei and the correction of the pandemonium effect unfortunately remains the dominant contribution in the final error of the *ab initio* approach. It is roughly estimated in the last column of the table based on the envelope of the various scenarios we tried and on the residues with respect to the reference ILL data.

D. Predictions of ^{238}U spectra

Since no experimental data on ^{238}U are available at the present time, we provide a prediction of its electron and antineutrino spectra using the above *ab initio* approach. This calculation was performed using our best data set as defined in Sec. III A. The ^{238}U spectrum is given in Table III after two irradiation periods into a neutron flux: 12 h, similar to the irradiation time of the ILL data, and 450 days as an approximation of a spectrum at equilibrium. All neutron-capture effects are turned off for this prediction, and the error budget described in Table II applies to this prediction. In Table III and for all subsequent tables showing spectra calculations, the quoted energy is at the center of a bin and the value of the spectrum is the mean values in that bin. Comparison with a previous estimate [20] is illustrated in Fig. 4. Despite some slight differences in shape, our work and previous predictions agree within $\pm 10\%$ across the full energy range. After multiplication with the β-inverse cross section [Eq. (10)], the net effect on the integrated detected neutrino flux is a 9.8% increase for the ^{238}U contribution.

TABLE II. Sources of errors in the ^{235}U electron spectrum as predicted by the *ab initio* approach. All errors are given in percent at 1σ (68% C.L.).

Kinetic E (MeV)	Nuclear databases	Forbid. treatment	$A_{C,W}$ corrections	Missing info.
2.00	1.2	0.2	0.1	10
2.25	1.3	0.2	0.2	10
2.50	1.3	0.1	0.3	10
2.75	1.3	0.1	0.3	10
3.00	1.4	0.4	0.4	10
3.25	1.6	0.7	0.5	10
3.50	1.7	0.1	0.5	10
3.75	1.9	1.3	0.6	10
4.00	2.2	1.6	0.6	10
4.25	2.5	1.6	0.7	10
4.50	2.8	1.4	0.8	10
4.75	3.2	1.0	0.8	10
5.00	3.8	0.5	0.9	10
5.25	4.4	0.2	0.9	10
5.50	5.2	0.2	0.9	15
5.75	6.1	0.2	0.9	15
6.00	7.1	0.2	1.0	15
6.25	8.0	0.3	1.0	15
6.50	9.0	0.4	1.1	15
6.75	10.1	0.4	1.1	15
7.00	10.9	0.5	1.1	20
7.25	11.0	0.7	1.1	20
7.50	10.7	0.8	1.1	>20
7.75	11.1	0.8	1.2	>20
8.00	13.3	1.2	1.3	>20

IV. IMPROVED CONVERSION OF REACTOR ELECTRON SPECTRA INTO ANTINEUTRINO

In the previous section we showed that the *ab initio* approach had strong limitations due to the unknown contribution from very unstable nuclei. Nevertheless we keep in mind that the β transitions described in nuclear databases represent about 90% of the total spectrum as measured at ILL. These physical

TABLE III. ^{238}U electron and antineutrino spectra obtained by combining our best compilation of data sets with the activity of all fission products as predicted by the MURE evolution code after a 12 h and 450 days irradiation time. Associated errors are those listed in Table II.

Kinetic E (MeV)	N_β (/fission/MeV)		$N_{\bar{\nu}_e}$ (/fission/MeV)	
	12 h	450 d	12 h	450 d
2.00	1.13	1.15	1.43	1.48
2.25	9.81(−1)	9.97(−1)	1.26	1.30
2.50	8.47(−1)	8.55(−1)	1.12	1.15
2.75	7.24(−1)	7.27(−1)	9.80(−1)	1.00
3.00	6.11(−1)	6.11(−1)	8.70(−1)	8.76(−1)
3.25	5.07(−1)	5.06(−1)	7.57(−1)	7.59(−1)
3.50	4.16(−1)	4.15(−1)	6.40(−1)	6.42(−1)
3.75	3.37(−1)	3.36(−1)	5.39(−1)	5.39(−1)
4.00	2.68(−1)	2.67(−1)	4.50(−1)	4.51(−1)
4.25	2.11(−1)	2.10(−1)	3.67(−1)	3.67(−1)
4.50	1.64(−1)	1.63(−1)	2.94(−1)	2.93(−1)
4.75	1.27(−1)	1.27(−1)	2.32(−1)	2.32(−1)
5.00	9.72(−2)	9.69(−2)	1.83(−1)	1.83(−1)
5.25	7.37(−2)	7.33(−2)	1.43(−1)	1.43(−1)
5.50	5.55(−2)	5.52(−2)	1.10(−1)	1.10(−1)
5.75	4.17(−2)	4.14(−2)	8.35(−2)	8.35(−2)
6.00	3.12(−2)	3.10(−2)	6.21(−2)	6.21(−2)
6.25	2.31(−2)	2.30(−2)	4.70(−2)	4.70(−2)
6.50	1.68(−2)	1.66(−2)	3.58(−2)	3.58(−2)
6.75	1.17(−2)	1.16(−2)	2.71(−2)	2.71(−2)
7.00	7.92(−3)	7.85(−2)	1.95(−2)	1.95(−2)
7.25	5.28(−3)	5.23(−2)	1.32(−2)	1.33(−2)
7.50	3.48(−3)	3.44(−2)	8.65(−3)	8.65(−3)
7.75	2.22(−3)	2.19(−2)	6.01(−3)	6.01(−3)
8.00	1.40(−3)	1.38(−2)	3.84(−3)	3.84(−3)

distributions of endpoints and nuclear charges are precious information for controlling the conversion between electron and antineutrino spectra. We describe below how this can be combined to very precise ILL electron data for an improved prediction of antineutrino spectra.

A. Previous conversion procedure

The measurements performed at ILL gave access only to the global electron spectrum of a fissile isotope, i.e., the sum of the contributions of all fission products. Thin target foils of fissile isotopes ^{235}U, ^{239}Pu, and ^{241}Pu were exposed to the thermal neutron flux 80 cm away from the center of the compact fuel assembly. A tiny part of the emitted electrons could exit the reactor core through a straight vacuum pipe to be detected by a high resolution iron-core electron spectrometer [13]. The electron rates were recorded by a point-wise measurement of the spectrum in magnetic field steps of 50 keV, providing an excellent determination of the shape of the electron spectrum with sub-percent statistical error. The published data are smoothed over 250 keV. Except for the highest energy bins with poor statistics, the dominant error was the absolute normalization, quoted around 3% (90% C.L.)

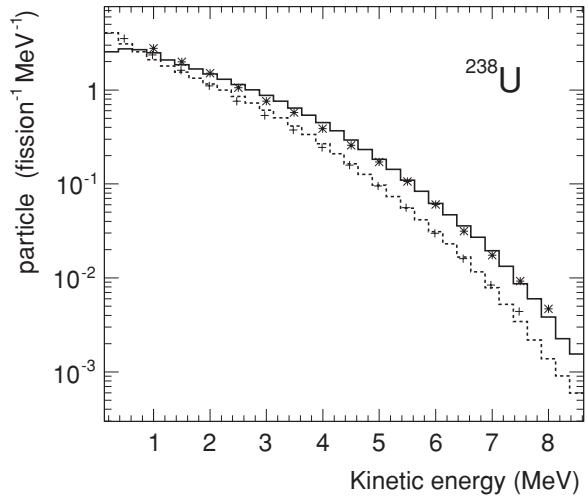

FIG. 4. *ab initio* calculation of the electron (dashed histogram) and antineutrino (solid histogram) spectra of ^{238}U for a 450 day irradiation time. For comparison the predictions of Ref. [20] for an infinite irradiation time are plotted as crosses for the electron spectrum and as stars for the antineutrino spectrum.

with weak energy dependence. Note also that the ILL spectra are taken after typically 1 day of irradiation, meaning that the longest lived β emitters (lowest energy β rays) have not reached equilibrium yet. These aspects are discussed in detail in Sec. V B.

The neutrino spectra, not directly detected, were deduced from those of the electron via a conversion procedure which induced some extra systematic effects. In Refs. [9–12] the authors considered 30 virtual β branches. The procedure consisted in dividing the electron spectrum into 30 slices. Starting with the highest energy slice, the few data points in this slice were used to fit the endpoint and branching ratio of the first virtual branch. The full contribution of this virtual branch (from endpoint down to zero energy) was then subtracted from the experimental spectrum and the procedure repeated for the next, lower energy, slice. Then the antineutrino spectrum was simply the sum of all fitted virtual branches, converted to antineutrino branches by replacing E_e by $E_\nu = E_0 - E_e$ and applying the correct radiative corrections. This procedure was repeated several times, describing the spectrum with somewhat different sets of endpoint energies. Possible steps in the shape induced by the relatively small number of virtual branches were smoothed out by taking the average of all spectra and merging the 50 keV bins into the 250 keV presented in the publications. The theoretical expression of a virtual branch was the same as Eq. (4), except for the A_C and A_W corrections which were treated at the very end as an effective linear correction to the final antineutrino spectra

$$\Delta N_\nu^{C,W}(E_\nu) \simeq 0.65\,(E_\nu - 4.00)\ \%, \tag{11}$$

with E_ν in MeV. The final error of the conversion procedure was estimated to be 3–4% (90% C.L.), to be added in quadrature with the electron calibration error.

In a recent paper [46], Vogel pointed out the main limitations of this conversion procedure. Despite the discontinuity of the Fermi function at the endpoint energy of an

antineutrino branch, the "true" antineutrino spectrum from fission fragment appears continuous because thousands of branches contribute with a quasicontinuous endpoint distribution. When describing the spectrum by only 30 virtual branches, a spurious oscillation with respect to the true spectrum appears around each virtual endpoint energy. Therefore smoothing out these oscillations requires sufficiently narrow slices of electron data and antineutrino energy bins several times larger than the slice width. All these criteria could not be fulfilled for the electron data taken at ILL, and the estimation of the remaining effects is part of the quoted error bar. The other criterion highlighted by Vogel was the knowledge of the average nuclear charge $\langle Z \rangle$ of the virtual branches as a function of their endpoint energy. This information turns out to be of crucial importance for the shape of the high energy part of the antineutrino spectrum.

B. Improvements of the conversion procedure

Our new conversion method allows us to address the sources of error in a complementary way. It consists in starting with our *ab initio* prediction of Sec. III and restrict the use of effective branches to fit only the missing few percent contribution of the difference with the reference ILL electron data. This way we keep the distributions of β branches very close to the physical one, and we can apply A_C and A_W corrections at the branch level. The reference ILL electron data are still fitted, but the contribution of unphysical virtual branches is reduced by an order of magnitude. We use all available data in ENSDF plus the above-mentioned 67 nuclei from the "pandemonium corrected" measurements. In the case of the data from Ref. [33], only the total β spectra of each nuclide are available, not the complete decay scheme as would be best. Hence, to be converted to a neutrino spectrum, each β spectrum measured must be fitted by a set of branches. These branches differ from the virtual branches used to fit the ILL data by the fact that in this work the nuclear charge is perfectly known. Moreover, the validation of the spectrum shape at the level of one nucleus provides a more refined description of the β-decay scheme equivalent to a small slice size in the total spectrum, pinning down the sources of errors discussed in Ref. [46].

On top of the contributions of all ENSDF and pandemonium corrected β branches, the missing contribution to match the ILL electron spectrum is fitted using a set of five effective β branches with a nuclear charge of $Z = 46$ (chosen as the average of the distribution of fission products), and assuming that transitions are allowed transitions. The normalization and the endpoint are two free parameters for each branch. Examples of the *ab initio* and fitted contributions of the ^{235}U electron spectrum are illustrated in Fig. 5 as stacked histograms. The residues of the fitted missing contribution are shown in Fig. 6(a). They are small, typically at the level of the statistical error of the ILL data, except in the 4.5–6.0 MeV range, where one can see an oscillation pattern with an amplitude reaching three times the error of the ILL data at maximum. This may point to a systematic effect due to a failure of the fit model. We checked that using more effective branches is not efficient because of the limited number of experimental points available. The impact of these nonstatistical residues in the final error is discussed latter.

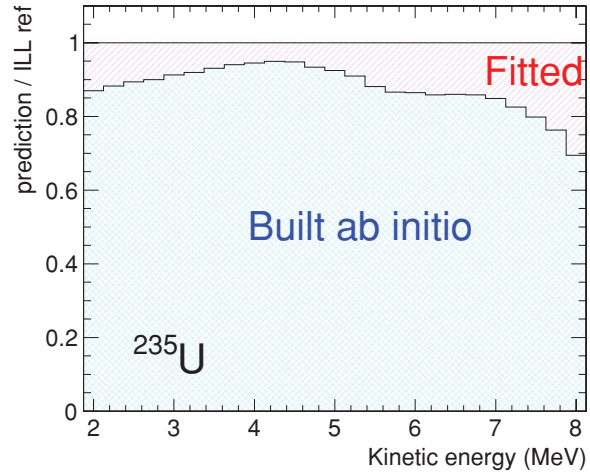

FIG. 5. (Color online) Lower (blue) double hatched area shows the contribution of our *ab initio* prediction (ENSDF + pandemonium corrected nuclei) relative to the ILL reference data. The missing contribution coming from unknown nuclei and remaining systematic effects of nuclear databases [upper (red) hatched area] is fitted using a set of five effective β branches.

C. New reference antineutrino spectra

Converting all branches from the nuclear databases plus the five fitted ones into antineutrino branches (as described in Sec. II), we obtain the predicted antineutrino spectrum. The residues with respect to the prediction of Schreckenbach *et al.* [10] are shown in Fig. 6(b). It exhibits a good agreement in shape but a mean normalization shift of about +3%. This shift of the emitted antineutrino flux is modulated at higher energy by oscillations which look like images of the oscillations in the electron residues. When folded with the β-inverse cross section, the predicted increase of detected antineutrino rate from ^{235}U is about 2.5%. Note that this positive shift is a mean value computed between the energy threshold (1.8 MeV) imposed by the detection process and infinity. The physical constraint of one emitted electron for one emitted antineutrino must still be fulfilled. We did check that the total integral of our electron spectrum fitted on the ILL reference and the integral of the associated converted neutrino spectrum were identical at the 10^{-4} level. Since all our individual β and antineutrino branches are normalized to the same integral with much higher accuracy, this result gives an estimate of the numerical precision in the sum of thousands of branches.

To test the validity of our procedure, we applied it to effective calculated electron and antineutrino spectra. This method was inspired by the work of Vogel [46]. We generated electron and antineutrino spectra as the sum of the spectra of all fission products indexed in ENSDF, weighted by the activity predicted by the MURE code after 12 h of irradiation. This way, our test β spectrum corresponds to the dashed-dotted curve of Fig. 3. We know from Sec. III that these spectra are

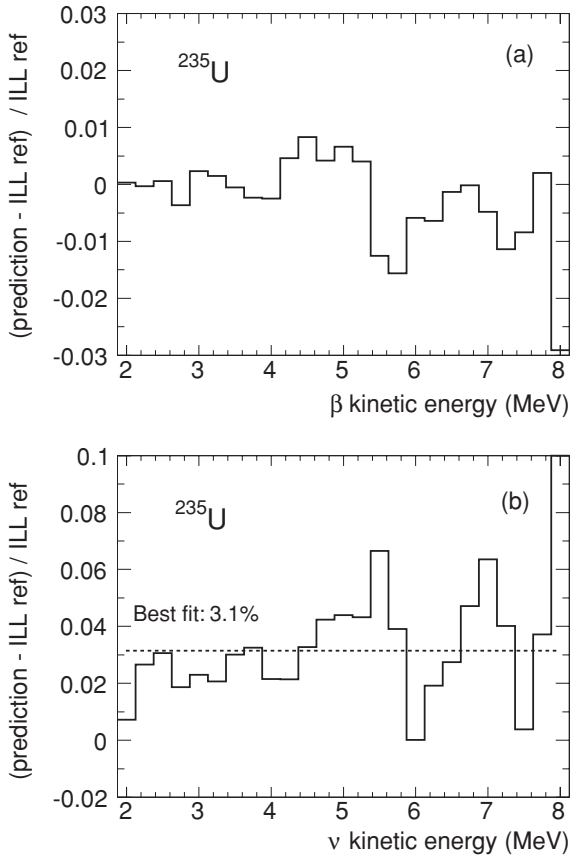

FIG. 6. Relative difference to ILL spectra [10] for electron (a) and antineutrino (b) spectra for ^{235}U. While electron residues are zeroed at the ±1% level by the fitting procedure, antineutrino residues exhibit a mean normalization shift of about 3% [dashed line in (b)].

close to the ones measured at ILL, and in the context of this test we call them "true" spectra in the sense that they are unambiguously connected to each other by the conversion of each single branch of the sum. Then we followed the exact same procedure as the one described in Refs. [10–12] to convert our true electron spectrum into an antineutrino spectrum. This includes using 30 virtual branches and the same effective Z distribution and the same effective $A_C + A_W$ correction [Eq. (11)]. The spectrum converted in this fashion is finally compared to our true antineutrino spectrum. Figure 7 shows that despite a very good fit quality of the electron spectrum (all electron residues are within a few 10^{-3} from 1 to 8 MeV), the converted antineutrino spectrum exhibits residues with oscillations of few percent amplitude around the endpoint of each fitted branch. As expected, rebinning smoothes out these oscillations (solid curve), but a residual $\simeq$+3% offset is clearly visible across the whole energy range. This curve can be directly compared to the result of our conversion of the ILL data, in Fig. 6(b). Very good agreement is found, validating the above-predicted deviation from the ILL antineutrino spectra.

Switching on and off the various ingredients of the ILL conversion reveals a twofold origin of the normalization shift. At low energy, the deviation is mainly due to the treatment of the A_C and A_W correction terms. In Eq. (6) these two terms

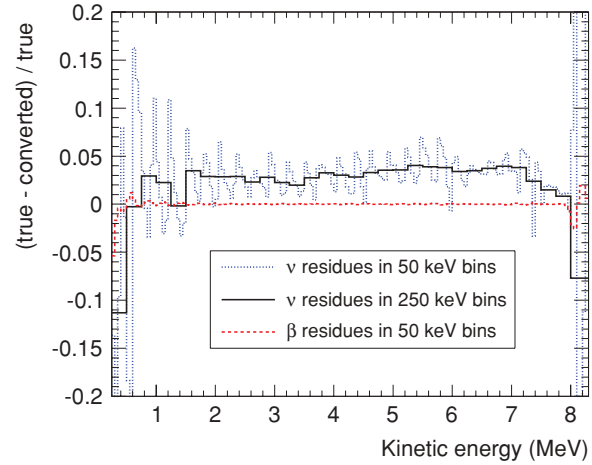

FIG. 7. (Color online) Independent cross-check of our results based on known reference spectra (pure ENSDF database). Dashed red line: electron residues after fitting with 30 virtual branches. Dotted blue line: relative difference between the reference antineutrino spectrum and the one converted according to the ILL procedure, in 50 keV bins. Smoothing out the residual oscillations in 250 keV bins (solid black line) exhibits the same 3% normalization shift as in Fig. 6(b).

appear multiplied by the energy, hence one would expect their net contribution to grow with energy. Nevertheless A_C itself has some hidden energy dependence via the Z distribution of all branches [Eq. (8)], while the estimate of A_W is a constant [Eq. (9)]. To illustrate the size of the total correction $A_C + A_W$, we show the ratio of corrected over noncorrected spectra in Fig. 8 in the case of total spectra buildup from all ENSDF branches. There is a linear trend at high energy, but a direct comparison with the effective linear correction used in the previous analysis [Eq. (11)] should not be made at this stage. In fact, in the conversion procedure, the electron spectrum is fitted on the electron ILL data. By definition, the fitting procedure optimizes the parameters of the few virtual electron branches

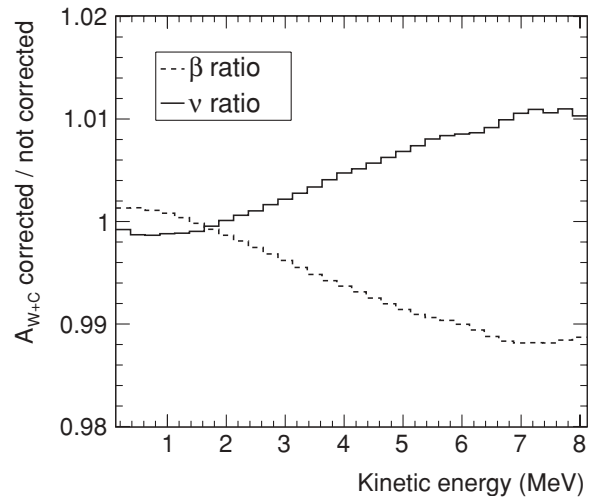

FIG. 8. Ratio of total spectra computed from all ENSDF branches with and without the A_C and A_W correction terms. The dashed (solid) curve shows the ratio of electron (neutrino) spectra.

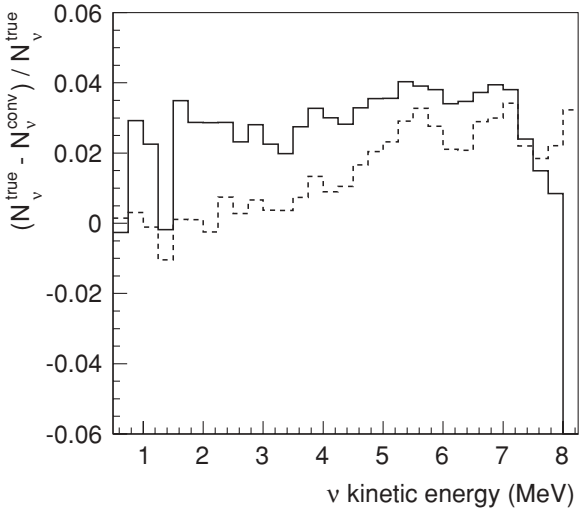

FIG. 9. The solid curve is the same solid curve as in Fig. 7. The dashed curve shows the relative difference between the reference "true" spectrum and the one converted according to the ILL procedure, but with the implementation of A_C and A_W corrections at the level of each virtual branch. This curve becomes close to the reference spectrum at lower energy and explains most of the +3% shift observed in Figs. 6(b) and 7 below 4 MeV.

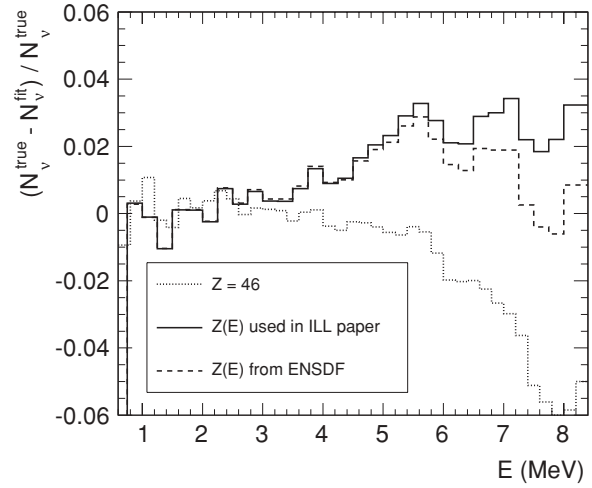

FIG. 10. Deviation from the true antineutrino spectrum induced by various $Z(E)$ functions used in the formula of the virtual branches. For this test A_C and A_W are turned off in the "true" branches as well as in the virtual branches. This effect takes over the +3% deviation observed in Figs. 6(b) and 7 above 4 MeV.

used in this work so that the total electron spectrum always matches the ILL data, whatever the correction terms included in the theoretical expression of the branches. Therefore in the conversion process, only the neutrino spectrum is sensitive to the A_C and A_W terms. The final effect is not intuitive but can be computed numerically as shown in Fig. 9. When applied at the branch level, the A_W and Z-dependent A_C corrections deviate from the effective formula of Eq. (11) and explain the predicted 3% shift in the low energy region. We stress that no improvement was brought to the theoretical expression of the corrections [Eqs. (8) and (9)], only the way of implementing these corrections has been revisited, avoiding the extra approximation of the effective correction of Eq. (11). We show that this approximation was giving too much amplitude to the negative correction in intensity at low energy. In fact the $A_C + A_W$ correction in our procedure is almost zero below 3 MeV and increases to about +2% at 7 MeV. The effect is large enough to explain the observed 3% shift at low energy.

At higher energy, the dominant source of the shift comes from the parametrization of the charge distribution associated with the virtual β branches. Figure 10 illustrates how large errors can be induced by the too rough approximation of a constant nuclear charge. In the ILL data analysis, the mean charge of each virtual branch was taken from a polynomial fit $Z(E_0)$ of the tabulated nuclear data [Eq. (3) of Ref. [10]]. This greatly reduced the bias, but still this approach does not take into account the very large dispersion of nuclear charges around this mean. Even a new $Z(E_0)$ function, fitted on the same data used to build our true spectrum generates a deviation of a few percent at high energy.

Further cross-checks of our results are based on minimizing the electron residues in different independent ways. First we checked that the new conversion procedure is not sensitive to the chosen starting point for the *ab initio* calculations. All the results presented above were obtained by adding five virtual branches to the spectrum built up from nuclear databases and using independent yields calculated after 12 h of irradiation time to match as closely as possible the experimental conditions at ILL. Figure 11 shows the variation of the neutrino residues when using independent yields at 36 h instead of 12 h or even cumulative fission yields, corresponding to the equilibrium regime reached after infinite irradiation time. One can see that the variations induced in the antineutrino

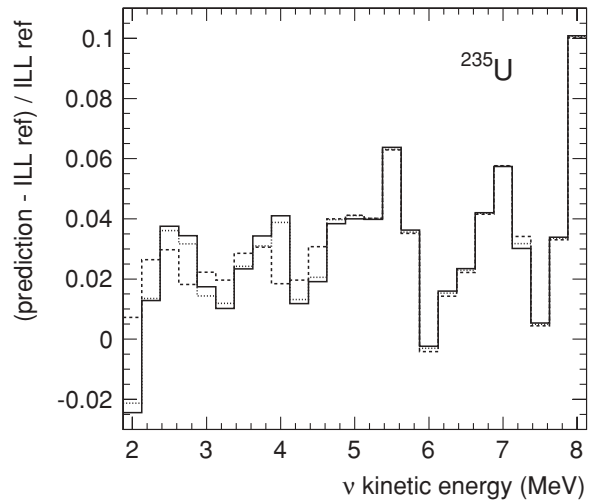

FIG. 11. Stability check of antineutrino residues when using different estimates of fission yields for the initial *ab initio* calculation [see Eq. (2)]: independent yields calculated via MURE after 12 h of irradiation (solid line), after 36 h (dotted line), and cumulative yields (dashed line). The difference between neutrino residues is less than 1% below 4.5 MeV and negligible for higher energies.

TABLE IV. Results of the new conversion procedure on the ^{235}U antineutrino spectrum. The electron residues between our prediction and ILL data [10] are given in percent as an indication of the quality of the fitting procedure. The antineutrino spectrum is normalized per fission and correspond to the spectrum for a 12 h irradiation time. All errors are given in percent at 1σ (68% CL).

E_{kin}	β res.	$N_{\bar{\nu}_e}$	Error ΔN_ν in % at 1σ level				
(MeV)	(%)	(/fission)	Stat.	Conv.	$A_{C,W}$	Norm.	Total
2.00	0.03	1.31	0.3	1.0	0.5	1.7	2.1
2.25	−0.03	1.11	0.3	1.0	0.5	1.7	2.1
2.50	0.07	9.27(−1)	0.3	1.0	0.5	1.7	2.1
2.75	−0.35	7.75(−1)	0.3	1.0	0.5	1.7	2.1
3.00	0.24	6.51(−1)	0.3	1.0	0.5	1.8	2.1
3.25	0.14	5.47(−1)	0.3	1.0	0.5	1.8	2.1
3.50	−0.06	4.49(−1)	0.3	1.0	1.0	1.8	2.3
3.75	−0.22	3.63(−1)	0.3	1.0	1.0	1.8	2.3
4.00	−0.19	2.88(−1)	0.3	1.0	1.0	1.8	2.3
4.25	0.52	2.27(−1)	0.3	1.5	1.0	1.8	2.6
4.50	0.89	1.77(−1)	0.3	1.5	1.0	1.8	2.6
4.75	0.46	1.37(−1)	0.3	1.5	1.0	1.8	2.6
5.00	0.70	1.09(−1)	0.3	1.5	1.5	1.8	2.8
5.25	0.43	8.54(−2)	0.3	1.5	1.5	1.8	2.8
5.50	−1.24	6.56(−2)	0.3	3.0	1.5	1.8	3.8
5.75	−1.56	4.99(−2)	0.3	3.0	2.0	1.8	4.1
6.00	−0.59	3.68(−2)	0.3	3.0	2.0	1.8	4.1
6.25	−0.62	2.74(−2)	0.3	3.0	2.0	1.9	4.1
6.50	−0.08	2.07(−2)	0.3	3.0	2.0	1.9	4.1
6.75	0.09	1.56(−2)	0.3	3.0	2.0	1.9	4.1
7.00	-0.27	1.11(−2)	0.4	3.0	2.0	1.9	4.1
7.25	−0.90	6.91(−3)	0.4	3.0	2.0	1.9	4.1
7.50	−0.93	4.30(−3)	0.5	3.0	2.5	1.9	4.4
7.75	−0.14	2.78(−3)	0.9	3.0	2.5	1.9	4.4
8.00	−1.18	1.49(−3)	1.8	3.0	2.5	1.9	4.7

spectra are negligible ($\leqslant$1%). This can be understood by the fact that although the different sets of fission yields do change the shape of the *ab initio* spectrum by a few percent, this change is absorbed by the virtual branches fitting the missing contribution with respect to the ILL electron spectrum. The underlying distributions of nuclear charges and endpoints remain very similar, leading to the same final residues. This illustrates how our mixed approach gets rid of the dominant errors of the *ab initio* approach.

To avoid the use of virtual branches, we also tried minimizing the electron residues by tweaking the input parameters of the *ab initio* calculation, namely, the distributions of branching ratios or endpoints or both at the same time. This technique makes sense only if the tweaking does not disturb too much the physical distributions. Therefore in the minimization procedure, we implemented limitations of typically 15% for the variation range of physical parameters. Electron residues of similar quality could be obtained in this way at low energy, but deviations of several percent could not be avoided above 5 MeV. As already observed in Fig. 6, any large residues pattern in the electron fit show up in the antineutrino residues, slightly shifted in kinetic energy and amplified by a factor of about 3. This behavior is used to estimate our error budget, summarized in Table IV. Even in the case of zero residues, we count the statistical error of the reference β spectrum as the minimum error of the converted antineutrino spectrum (column 4). Based on our numerous tests of fitting methods, the amplified envelope of nonstatistical electron residues is added in quadrature as an extra conversion error (column 5).

In column 6, the error due to the $A_{C,W}$ terms is computed by propagating a 100% relative uncertainty through the conversion procedure. Thus the error budget shown is essentially the correction itself. We checked that the error envelope determined this way was largely including the change induced by the use of another expression of the correction found in Ref. [17]. Finally, the normalization error of the ILL reference data is directly propagated as a normalization error of the converted antineutrino spectrum (column 7). The total error is taken as the quadratic sum of all previous sources of errors. In the perspective of neutrino oscillation analyses, it is mandatory to consider the correlations between energy bins. The statistical and conversion errors are driven by random processes. Therefore they do not induce any bin-to-bin correlation. The normalization error of the ILL data should be treated as fully correlated over the whole energy range. Regarding the $A_{C,W}$ terms, we observe that they are propagated as a linear correction to the converted antineutrino spectrum above 4 MeV. The uncertainty on the slope coefficient fully correlates all high energy bins. Below 4 MeV the precise determination of the correlations would require dedicated

TABLE V. Results of the new conversion procedure on ^{239}Pu (1.5 days irradiation time) and ^{241}Pu (1.8 days irradiation time) antineutrino spectra; see comments for ^{235}U. The conversion error and the error due to the $A_{C,W}$ terms are the same as those in Table IV. The statistical and normalization errors for both plutonium isotopes can be found in Ref. [12].

$E_{\rm kin}$	^{239}Pu			^{241}Pu		
(MeV)	β res (%)	$N_{\bar{\nu}_e}$ (/fission)	$\Delta N_{\bar{\nu}_e}$ (%)	β res (%)	$N_{\bar{\nu}_e}$ (/fission)	$\Delta N_{\bar{\nu}_e}$ (%)
2.00	−0.03	1.13	2.3	−0.04	1.27	2.2
2.25	−0.12	9.19(−1)	2.3	0.10	1.07	2.2
2.50	0.14	7.28(−1)	2.4	−0.11	9.06(−1)	2.2
2.75	−0.38	6.13(−1)	2.4	0.00	7.63(−1)	2.2
3.00	0.31	5.04(−1)	2.4	0.24	6.39(−1)	2.2
3.25	0.05	4.10(−1)	2.4	0.98	5.31(−1)	2.2
3.50	0.04	3.21(−1)	2.6	0.65	4.33(−1)	2.4
3.75	1.49	2.54(−1)	2.6	0.49	3.51(−1)	2.4
4.00	−0.87	2.00(−1)	2.7	−0.09	2.82(−1)	2.5
4.25	−0.63	1.51(−1)	2.9	0.02	2.18(−1)	2.7
4.50	4.49	1.10(−1)	3.0	−1.26	1.65(−1)	2.8
4.75	0.21	7.97(−2)	3.0	−0.80	1.22(−1)	2.8
5.00	−2.47	6.15(−2)	3.3	−0.48	9.59(−2)	3.1
5.25	−2.48	4.68(−2)	3.3	−0.92	7.36(−2)	3.1
5.50	−5.41	3.50(−2)	4.4	−0.93	5.52(−2)	4.3
5.75	−0.32	2.55(−2)	4.6	−0.07	4.01(−2)	4.5
6.00	2.26	1.82(−2)	4.9	1.69	2.81(−2)	4.7
6.25	1.53	1.32(−2)	5.0	0.77	2.04(−2)	4.7
6.50	−0.76	9.82(−3)	5.2	0.10	1.50(−2)	4.9
6.75	5.47	7.32(−3)	5.2	−0.94	1.07(−2)	4.9
7.00	−5.01	5.13(−3)	7.1	−0.32	7.20(−3)	5.3
7.25	−1.73	3.15(−3)	9.2	−1.23	4.47(−3)	5.3
7.50	−8.94	1.83(−3)	11.1	−0.96	2.54(−3)	5.7
7.75	−32.75	1.03(−3)	15.7	−1.07	1.65(−3)	5.7
8.00	−55.56	4.91(−4)	20.6	−1.55	9.63(−4)	7.0

numerical studies, but in that energy domain the size of the $A_{C,W}$ corrections and their errors are small and have negligible impact in the error budget.

We applied our same conversion procedure to plutonium isotopes. Results are given in Table V. The conclusions given for the ^{235}U antineutrino spectrum remain valid for these isotopes. The main net effect is a mean $\approx$+3% normalization shift with respect to previous reference spectra. The equivalent increase in the detected neutrino spectrum is 3.1% for ^{239}Pu and 3.7% for ^{241}Pu.

V. CONTEXT OF REACTOR NEUTRINO EXPERIMENTS

A. A useful phenomenological parametrization

A phenomenological parametrization of our fission antineutrino spectra could be useful for sensitivity studies requiring different binning or energy domains than those proposed in Tables III–V. Therefore, as in Ref. [47], we provide a parametrization of the spectrum of a given isotope using the exponential of a polynomial

$$S_{k,\rm fit}(E_\nu) = \exp\left(\sum_{p=1}^{6} \alpha_{pk} E_\nu^{p-1}\right), \tag{12}$$

with the coefficients α_{pk} determined by a fit to the data using the MIGRAD algorithm of the TMINUIT ROOT class [48]. To this aim, we minimize the χ^2 function

$$\chi^2 = \sum_{i,j} D_i V_{ij}^{-1} D_j,$$
$$\text{with } D_i \equiv \sum_{p=1}^{6} \alpha_{pk}\left(E_\nu^{(i)}\right)^{p-1} - \ln S_k^{(i)}, \tag{13}$$

where $E_\nu^{(i)}$ and $S_k^{(i)} \equiv S_k(E_\nu^{(i)})$ are the values of the antineutrino energy and the corresponding antineutrino spectrum, respectively, provided in Tables III–V. Since we are fitting the logarithm of the flux, the covariance matrix V_{ij} contains the relative errors of the $S_k^{(i)}$. For the diagonal element V_{ii} we take the total error quoted in the above-mentioned tables. Because the error of the ^{238}U spectrum has been estimated from the envelope of all systematic effects of the nuclear databases, we assume no bin-to-bin correlation. For our new converted spectra, the fully correlated errors on the absolute calibration of ILL β spectra and on the $A_{C,W}$ correction terms contribute to the off-diagonal elements of the covariance matrix as

$$V_{ij} = \sigma_i^{\rm cal}\sigma_j^{\rm cal} + \sigma_i^{\rm corr}\sigma_j^{\rm corr} \quad i \neq j. \tag{14}$$

The plots in Figs. 12(a)–12(d) show the resulting spectra for the six parameter fits in comparison to the data and the corresponding χ^2 values per degree of freedom. The best goodness-of-fit is obtained with polynomial of order 5. The plots in Figs. 12(e)–12(h) show the residues of the fit in units of σ_i, where the error is obtained from the covariance matrix V by $\sigma_i = S_k^{(i)}\sqrt{V_{ii}}$. Note that in case of correlations between the $S_k^{(i)}$ these residuals do not add up to the total χ^2. All antineutrino spectra are very well described by the chosen phenomenological parametrization of Eq. (12). The best fit coefficients α_{pk} and their correlation matrices are given in Table VI. We can see quite large anticorrelations among consecutive fit parameters which could be induced by the choice of the exponential of a polynomial for the fit function. Therefore one should be aware of possible bias in the propagation of correlations when using these fits, whereas it is a practical way to compute nominal spectra.

B. Off-equilibrium corrections

The ILL spectra were acquired after a quite short irradiation time in a quasipure thermal neutron flux, between 12 h and 1.8 days depending on the measured isotopes. For neutrino reactor experiments, the irradiation time scale would rather be a reactor cycle duration, typically 1 yr. Among the fission products, about 10% of them have a β-decay lifetime long enough to keep accumulating after several days, some of them presenting sufficient large capture cross sections to possibly affect the final inventory. Moreover, in a standard Pressurized Water Reactor (PWR), the neutron energy spectrum exhibits more

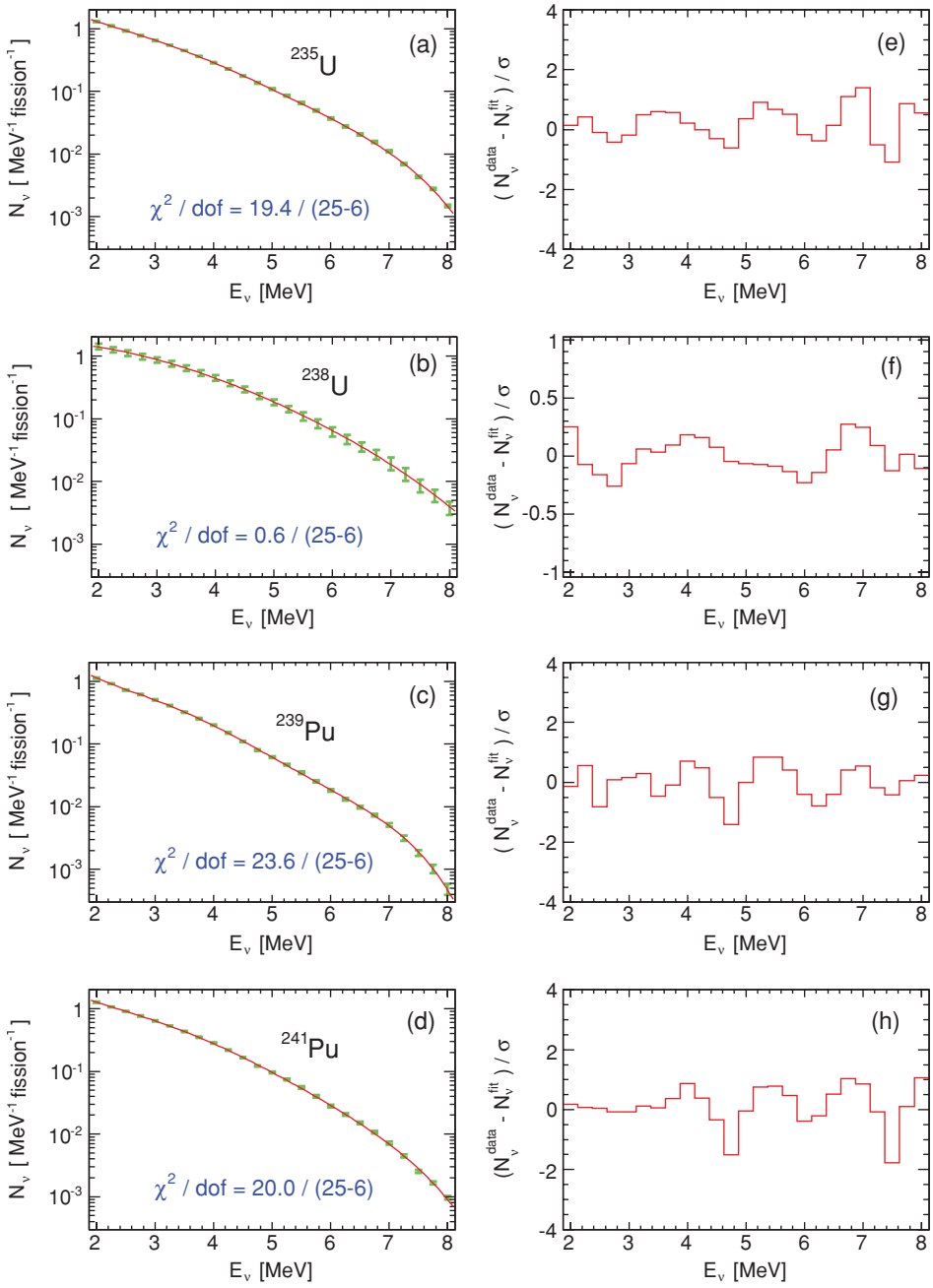

FIG. 12. (Color online) Fit of the antineutrino spectra predicted in this work. The red curves in the left panels correspond to a six-parameter fit (polynomial of order 5). Also shown are the data with their 1σ error bars and the χ^2 per degree of freedom. The right panels show the residuals of the fits.

important epithermal and fast neutron energy components than in the ILL measurements. These higher energy components of the neutron flux add small contributions to the fissions of ^{235}U (as well as for the other fissioning isotopes) leading to different distributions of the fission products. In this section we study the effect of these phenomena on the reference neutrino spectra and compute the associated corrections. Since these corrections are relative deviations between spectra at different irradiation times, we assume they are pretty insensitive to the sources of error of our *ab initio* calculations discussed in Sec. III.

Therefore the study was done with the MURE simulation of a PWR assembly of N4 type exhibiting a moderation ratio equal to that of a PWR core in order to represent the full reactor neutronic conditions. The infinite multiplication coefficient of the simulation has been successfully compared with similar simulations performed with the deterministic code DRAGON for French PWRs [49]. This simulation represents thus very well the real physical conditions of a reactor core. The condition of a constant power is assumed, renormalizing the neutron flux at each time step in order to compensate for the fuel burnup. We adapted the code in order to compute and store the amount of all β^- emitters produced over time [50]. In our simulation, the fission yields from the JEFF3.1.1 nuclear data library [45] were used. The yields coming from the 25 meV, 400 keV, and 14 MeV libraries were weighted by the fission rates in each

TABLE VI. Coefficients α_{pk} of the polynomial of order 5 for antineutrino flux from elements $k = {}^{235}$U, ^{238}U, ^{239}Pu, and ^{241}Pu. In the column $\delta\alpha_{pk}$. the 1σ errors on α_{pk} are given. Furthermore the correlation matrix of the errors is shown.

	$k = {}^{235}$U		Correlation matrix $\rho^k_{pp'}$					
p	α_{pk}	$\delta\alpha_{pk}$	1	2	3	4	5	6
1	3.217	4.09(−2)	1.00	−0.86	0.60	0.07	−0.17	−0.14
2	−3.111	2.34(−2)	−0.86	1.00	−0.84	0.12	0.25	0.01
3	1.395	4.88(−3)	0.60	−0.84	1.00	−0.56	−0.19	0.24
4	−3.690(−1)	6.08(−4)	0.07	0.12	−0.56	1.00	−0.42	−0.14
5	4.445(−2)	7.77(−5)	−0.17	0.25	−0.19	−0.42	1.00	−0.77
6	−2.053(−3)	6.79(−6)	−0.14	0.01	0.24	−0.14	−0.77	1.00
	$k = {}^{238}$U		Correlation matrix $\rho^k_{pp'}$					
p	α_{pk}	$\delta\alpha_{pk}$	1	2	3	4	5	6
1	4.833(−1)	1.24(−1)	1.00	−0.86	0.20	0.30	0.08	−0.27
2	1.927(−1)	5.86(−2)	−0.86	1.00	−0.58	−0.21	0.04	0.23
3	−1.283(−1)	1.11(−2)	0.20	−0.58	1.00	−0.48	−0.17	0.20
4	−6.762(−3)	1.92(−3)	0.30	−0.21	−0.48	1.00	−0.36	−0.20
5	2.233(−3)	2.84(−4)	0.08	0.04	−0.17	−0.36	1.00	−0.77
6	−1.536(−4)	2.86(−5)	−0.27	0.23	0.20	−0.20	−0.77	1.00
	$k = {}^{239}$Pu		Correlation matrix $\rho^k_{pp'}$					
p	α_{pk}	$\delta\alpha_{pk}$	1	2	3	4	5	6
1	6.413	4.57(−2)	1.00	−0.86	0.60	0.10	−0.17	−0.13
2	−7.432	2.85(−2)	−0.86	1.00	−0.84	0.08	0.25	−0.01
3	3.535	6.44(−3)	0.60	−0.84	1.00	−0.54	−0.20	0.26
4	−8.820(−1)	9.11(−4)	0.10	0.08	−0.54	1.00	−0.45	−0.08
5	1.025(−1)	1.38(−4)	−0.17	0.25	−0.20	−0.45	1.00	−0.79
6	−4.550(−3)	1.29(−5)	−0.13	−0.01	0.26	−0.08	−0.79	1.00
	$k = {}^{241}$Pu		Correlation matrix $\rho^k_{pp'}$					
p	α_{pk}	$\delta\alpha_{pk}$	1	2	3	4	5	6
1	3.251	4.37(−2)	1.00	0.87	−0.60	−0.08	0.17	0.13
2	−3.204	2.60(−2)	0.87	1.00	−0.84	0.11	0.25	−0.00
3	1.428	5.66(−3)	−0.60	−0.84	1.00	−0.56	−0.19	0.26
4	−3.675(−1)	7.49(−4)	−0.08	0.11	−0.56	1.00	−0.43	−0.11
5	4.254(−2)	1.02(−4)	0.17	0.25	−0.19	−0.43	1.00	−0.78
6	−1.896(−3)	9.03(−6)	0.13	0.00	0.26	−0.11	−0.78	1.00

neutron energy region. This simulation was compared with independent calculations using the FISPACT code [51] based on the European Activation File (EAF) nuclear data library, which just evolves the isotopic concentrations over time. A constant mean neutron flux of 3×10^{14} neutrons/(cm^2 s) was used for the FISPACT calculations.

The departures from our reference spectra are displayed as a function of time in Table VII for some relevant low energy bins. As expected, the accumulation of long-lived nuclei shows up as positive deviation which amplitude decreases with the neutrino energy and becomes negligible above 3.5 MeV. At the threshold of the β-inverse process, it takes about 100 days of irradiations for the antineutrino spectrum to be stable at the 1% level. Noting that the irradiation time for the reference spectrum of ^{235}U is 12 h instead of 36 h as for ^{239}Pu and ^{241}Pu, the corrections are similar for all isotopes. We checked with our evolution codes that the effects of neutron capture on the fission products as well as the contribution of the neutron spectrum above the thermal energy domain have small impact on the off-equilibrium corrections. Other tests were performed with the FISPACT code, showing that these results may depend on the system (neutron, flux and energy spectrum, geometry) used in the calculation. The error envelope covering our different results is of 30% on the total off-equilibrium corrections. Therefore the results quoted in Table VII should be taken as typical corrections at an N4 reactor. For applications with significantly different neutron flux or fuel geometry, dedicated simulations should be carried out for an accurate correction of the lowest energy bins of the antineutrino spectrum.

Off-equilibrium effects have independently been evaluated for the analysis of the Chooz experiment [52], which measured the neutrino spectrum of the two N4 reactors of the Chooz site. In this reference, the departure from the antineutrino ILL spectra were computed using the cumulative yields of some

TABLE VII. Relative off-equilibrium correction (in %) to be applied to the reference antineutrino spectra listed in Tables IV and V, for several energy bins and several irradiation times significantly longer than the reference times (12 h for U and 36 h for Pu); 1E7 = 1×10^7. Effect of neutron capture on fission products are included and computed using the simulation of a PWR fuel assembly with the MURE code.

			^{235}U		
	2.0 MeV	2.5 MeV	3.0 MeV	3.5 MeV	4.0 MeV
36 h	3.1	2.2	0.8	0.6	0.1
100 d	4.5	3.2	1.1	0.7	0.1
1E7 s	4.6	3.3	1.1	0.7	0.1
300 d	5.3	4.0	1.3	0.7	0.1
450 d	5.7	4.4	1.5	0.7	0.1
			^{239}Pu		
	2.0 MeV	2.5 MeV	3.0 MeV	3.5 MeV	4.0 MeV
100 d	1.2	0.7	0.2	<0.1	<0.1
1E7 s	1.3	0.7	0.2	<0.1	<0.1
300 d	1.8	1.4	0.4	<0.1	<0.1
450 d	2.1	1.7	0.5	<0.1	<0.1
			^{241}Pu		
	2.0 MeV	2.5 MeV	3.0 MeV	3.5 MeV	4.0 MeV
100 d	1.0	0.5	0.2	<0.1	<0.1
1E7 s	1.0	0.6	0.3	<0.1	<0.1
300 d	1.6	1.1	0.4	<0.1	<0.1
450 d	1.9	1.5	0.5	<0.1	<0.1

known long-lived fission fragments. The results are shown as markers in Fig. 13 to be compared with the histograms of our calculations. The overall agreement is good, even when evolving the spectrum back to an irradiation time as short as 10^4 s, where the corrections become quite large and have steep variations in time.

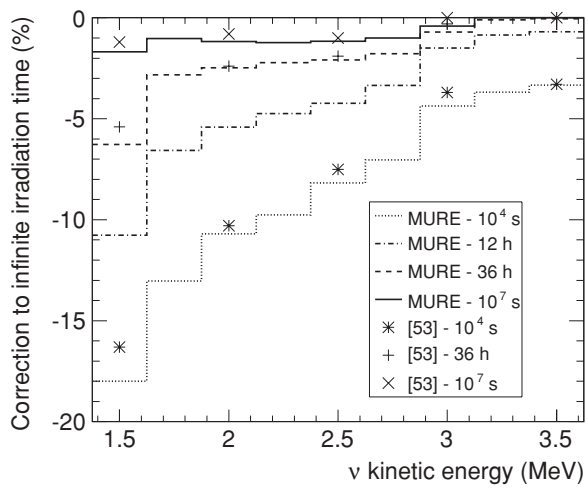

FIG. 13. Variations of the ^{235}U antineutrino spectrum for different irradiation times with respect to a reference spectrum considered at equilibrium.

Note that our reference spectrum at equilibrium does not use cumulative yields. Instead it is computed by our evolution code using independent fission yields and a long irradiation time. In the analysis of cumulative yields, it is in fact assumed that all nuclei have reached equilibrium. This is fully justified for short-lived fission products, whereas there is some ambiguity with the decay products of the longest half-lives. To avoid apparent double counting of the cumulative yields of the daughters, some very long-lived decays have been removed from the cumulative yield databases, but some are still present in the libraries. Because of these problems, it is recommended by nuclear databases [53] as a safer method to use independent yields with an inventory code. We have considered 450 days of irradiation as our reference to account for a spectrum that would have reached quasiequilibrium. In addition, this duration corresponds to a typical irradiation time of a fuel assembly in a PWR core.

Off-equilibrium effects where also computed in Ref. [54] where the authors used β branches of 571 fission fragments. The fission yields were taken from Ref. [55] and β decay properties came from experimental data. Our results are compatible with theirs considering the quoted uncertainties and the possible discrepancies in the neutron energy spectrum and flux used in the calculations. Note also that small additional discrepancies could arise from the smaller number of fission products used in the calculation of Kopeikin *et al.* [54].

In conclusion, our new reference spectra presented in Sec. IV are, strictly speaking, valid only for irradiation times comparable to the ones used at ILL for their measurement. For longer irradiations, corrections to these spectra are listed in Table VII. The above comparison between independent estimates suggests that the systematic errors associated with these corrections are at the sub-percent level relative to the total antineutrino spectrum.

C. Impact on published measurements

The new conversion of the ILL data described in Sec. IV leads to a 2.5% increase of the detected antineutrino flux, while the predicted shape is basically unchanged. The impact of this correction on the analysis of published measurements of antineutrino oscillations at reactor is discussed by the authors in a separate article [56]. The sensitivity of forthcoming reactor experiments is also updated in this context.

VI. CONCLUSION

Using all available data on fission yields and β decays of fission products, we have shown that *ab initio* calculations of total β spectra agreed with the reference ILL β spectra at the 10% level, illustrating the tremendous amount of nuclear data collected today. From this work, we gave a prediction of the antineutrino spectrum associated with the fission of ^{238}U with estimated relative uncertainty increasing from 10 to 20% with energy in the 2–8 MeV range. Since this isotope contributes to about 10% of the total fission

rate of a reactor, such a prediction is valuable. However, for the dominant isotopes, the remaining systematic errors of nuclear databases as well as the contribution of poorly known β transitions still prevent the *ab initio* approach from any use for high precision neutrino oscillation experiments at reactors.

This motivated the development of a new mixed approach combining the accurate reference of the ILL electron spectra with the physical distribution of β branches provided by the nuclear databases. We presented how this method gets rid of the main systematic error of the *ab initio* approach, allowing better control of the conversion of reference electron spectra into antineutrino spectra. While the final error budget ended up being comparable to that of previous reference work [10–12], we demonstrated that the antineutrino spectra emitted by the fission of ^{235}U, ^{239}Pu, and ^{241}Pu isotopes have to be corrected for a systematic shift of about 3% in normalization. This net effect was presented as the combination of an improved implementation of finite size corrections to the Fermi theory plus a more realistic description of the distribution of β branches.

ACKNOWLEDGMENTS

We are grateful to M. Cribier for instigating this work. M. Fallot would like to thank J. Wilson and O. Méplan for their availability and many useful discussions about the MURE code.

[1] C. Bemporad, G. Gratta, and P. Vogel, Rev. Mod. Phys. **74**, 297 (2002).
[2] Th. Lasserre and H. W. Sobel, C.R. Acad. Sci. Ser. B **6**, 749 (2005).
[3] F. Ardellier *et al.*, arXiv:hep-ex/0606025.
[4] X. Guo *et al.*, arXiv:hep-ex/0701029.
[5] J. K. Ahn *et al.*, arXiv:1003.1391.
[6] Yu. Klimov *et al.*, At. Energ. **76**, 123 (1994); V. A. Korovkin *et al.*, *ibid.* **65**, 712 (1988).
[7] N. S. Bowden *et al.*, Nucl. Instrum. Methods A **572**, 985 (2007); A. Bernstein *et al.*, J. Appl. Phys. **103**, 074905 (2008); N. S. Bowden *et al.*, *ibid.* **105**, 064902 (2009).
[8] A. Porta *et al.*, J. Phys. Conf. Ser. **203**, 012092 (2010).
[9] K. Schreckenbach *et al.*, Phys. Lett. B **99**, 251 (1981).
[10] K. Schreckenbach *et al.*, Phys. Lett. B **160**, 325 (1985).
[11] F. von Feilitzsch, A. A. Hahn, and K. Schreckenbach, Phys. Lett. B **118**, 162 (1982).
[12] A. A. Hahn *et al.*, Phys. Lett. B **218**, 365 (1989).
[13] W. Mampe *et al.*, Nucl. Instrum. Methods **154**, 127 (1978).
[14] A. Sirlin, Phys. Rev. **164**, 1767 (1967).
[15] P. Vogel, Phys. Rev. D **29**, 1918 (1984).
[16] N. B. Gove and M. J. Martin, At. Data Nucl. Data Tables **10**, 210 (1971).
[17] B. Holstein, Phys. Rev. C **9**, 1742 (1974).
[18] K. Takahashi, Prog. Theor. Phys. **45**, 1466 (1971).
[19] F. T. Avignone III and Z. D. Greenwood, Phys. Rev. C **22**, 594 (1980).
[20] P. Vogel, G. K. Schenter, F. M. Mann, and R. E. Schenter, Phys. Rev. C **24**, 1543 (1981).
[21] H. V. Klapdor and J. Metzinger, Phys. Lett. B **112**, 22 (1982).
[22] K. Zuber, arXiv:nucl-ex/0511009v1.
[23] B. R. Davis, P. Vogel, F. M. Mann, and R. E. Schenter, Phys. Rev. C **19**, 2259 (1979).
[24] N. H. Haag, Bestimmung des Antineutrinospektrums der Spaltprodukte von ^{238}U, Diplomarbeit, Technische Universität München, July 2008.
[25] [http://www.nndc.bnl.gov/ensdf/].
[26] H. Behrens and L. Szybisz, Shapes of Beta Spectra, Zentrale Für Atomkernenergie-Dokumentation (ZAED), Physics Data 6-1, 1976 (unpublished).
[27] O. Meplan *et al.*, in Proceedings of the ENC 2005, European Nuclear Conference, Nuclear Power for the XXIst Century: From Basic Research to High-Tech Industry, France (unpublished).
[28] J. F. Briesmeister, LANL Report No. LA-13709-M, 2000 (unpublished).
[29] Nuclear Energy Agency, Program Package NEA-1845 MURE [http://www.nea.fr/tools/abstract/detail/nea-1845].
[30] M. Fallot *et al.*, in Proceedings of the International Conference GLOBAL 2009: The Nuclear Fuel Cycle: Sustainable Options and Industrial Perspectives, Paper No. 9272 (unpublished).
[31] V. I. Kopeikin, Phys. At. Nucl. **66**, 472 (2003) [Yad. Fiz. **66**, 500 (2003)].
[32] J. C. Hardy *et al.*, Phys. Lett. B **71**, 307 (1977); J. C. Hardy, B. Jonson, and P. G. Hansen, *ibid.* **136**, 331 (1984).
[33] O. Tengblad *et al.*, Nucl. Phys. A **503**, 136 (1989); G. Rudstam *et al.*, At. Data Nucl. Data Tables **45**, 239 (1990).
[34] R. C. Greenwood *et al.*, Nucl. Instrum. Methods A **314**, 514 (1992).
[35] A. Algora and J. L. Tain (private communication).
[36] J. L. Tain *et al.*, in Proceedings of the International Conference on Nuclear Data for Science and Technology, Jeju Island, Korea, April, 2010 (unpublished).
[37] J. Katakura, T. Yoshida, K. Oyamatsu, and T. Tachibana, JENDL Fission Product Decay Data File 2000, JAERI Report No. 1343 (unpublished).
[38] K. Takahashi, M. Yamada, and T. Kondoh, At. Data Nucl. Data Tables **12**, 101 (1973) and references therein.
[39] J. Katakura, T. Yoshida, K. Oyamatsu and T. Tachibana, J. Nucl. Sci. Technol. **38**, 470 (2001).
[40] T. Yoshida *et al.*, J. Nucl. Sci. Technol. **36**, 135 (1999).
[41] A. Algora *et al.*, in *Proceedings of the International Conference on Nuclear Data for Science and Technology, 2007* (EDP Sciences, Nice, France, 2008), pp. 43–46.
[42] D. Cano-Ott *et al.*, Nucl. Instrum. Methods A **430**, 488 (1999); **430**, 333 (1999); J. L. Tain *et al.*, *ibid.* **571**, 728 (2007); **571**, 719 (2007).
[43] Proposal to the PAC of the JYFL Accelerator Laboratory "Study of nuclei relevant for precise predictions of reactor neutrino spectra," spokespersons: M. Fallot, A. Algora, and J. L. Tain (unpublished).

[44] A. Algora *et al.*, Phys. Rev. Lett. **105**, 202501 (2010).
[45] [http://www.nea.fr/html/dbdata/JEFF/index-JEFF3.1.1.html].
[46] P. Vogel, Phys. Rev. C **76**, 025504 (2007).
[47] P. Huber and T. Schwetz, Phys. Rev. D **70**, 053011 (2004).
[48] [http://root.cern.ch/root/html/TMinuit.html].
[49] J. Le Mer, Mémoire dès Sciences Appliquées (Génie Energétique), Université de Montréal, Ecole Polytechnique de Montréal, Sept. 2007.
[50] M. Fallot *et al.*, in *Proceedings of the International Conference on Nuclear Data for Science and Technology, 2007* (EDP Sciences, Nice, France, 2008), p. 1273.
[51] [http://www.fusion.org.uk/techdocs/ukaea-fus-534.pdf].
[52] M. Apollonio *et al.*, Phys. Lett. B **466**, 415 (1999); Eur. Phys. J. C **27**, 331 (2003).
[53] IAEA-TECDOC-1168, Dec. 2000 (unpublished), [http://www-nds.iaea.org/reports-new/tecdocs/iaea-tecdoc-1168.pdf].
[54] V. I. Kopeikin, L. A. Mikaelyan, and V. V. Sinev, Phys. At. Nucl. **67**, 11 (2004); **67**, 1963 (2004).
[55] T. R. England and B. F. Rider, Los Alamos National Laboratory, LA-UR-94-3106, 1993 (unpublished); ENDF-349, 1993 (unpublished).
[56] G. Mention *et al.*, arXiv:1101.2755.